LXR Regulates Cholesterol Uptake Through Idol-Dependent Ubiquitination of the LDL Receptor

Noam Zelcer*, et al.*

5-hydroxytryptamine, *o*-methoxylphenylethylamine, phenylethylamine, tryptamine. All chemicals were purchased from Sigma and tested at 1 mM concentrations, except for the FLRFamide and FMRFamide peptides, which were tested at 10 μM.

13. C. N. Connolly, K. A. Wafford, *Biochem. Soc. Trans.* **32**, 529 (2004).
14. T. Okuda *et al.*, *Nat. Neurosci.* **3**, 120 (2000).
15. K. Kusano, R. Miledi, J. Stinnakre, *J. Physiol.* **328**, 143 (1982).
16. For ion replacement experiments, oocytes expressing LGC-40, LGC-53, or LGC-55 were held at a resting potential of −90 mV. LGC-40, LGC-53, or LGC-55 currents were evoked with 2 μM choline, 5 μM dopamine, and 5 μM tyramine, respectively, in ND96 medium, sodium-free medium (96 mM cholineCl or NMDG-Cl replacing NaCl) or low-chloride medium (96 mM NaGluconate replacing NaCl). After 5 s, a voltage ramp of 20 mV/s from −90 mV to +60 mV was applied. Currents from voltage ramps recorded in the absence of ligands were subtracted from these current traces.
17. M. J. Alkema, M. Hunter-Ensor, N. Ringstad, H. R. Horvitz, *Neuron* **46**, 247 (2005).
18. Descriptions of *lgc-55* rescuing transgenes and the *lgc-55* reporter transgene are in (*9*).
19. J. White, E. Southgate, J. N. Thompson, S. Brenner, *Philos. Trans. R. Soc. London B Biol. Sci.* **314**, 1 (1986).
20. *lgc-40* and *lgc-53* mutants were grossly normal in locomotion, egg laying, defecation, and pharyngeal pumping. We also tested *lgc-53* mutants for defects in slowing in response to detection of a bacterial food source and for resistance to exogenous dopamine in locomotion and egg-laying assays. For experimental details, see (*9*).
21. K. A. Green, G. A. Cottrell, *Pfluegers Arch.* **434**, 313 (1997).
22. N. S. Magoski, A. G. M. Bulloch, *J. Neurophysiol.* **81**, 1330 (1999).
23. T. I. Webb, J. W. Lynch, *Curr. Pharm. Des.* **13**, 2350 (2007).
24. And references in ref. (*27*).
25. G. I. Hatton, Q. Z. Yang, *J. Neurosci.* **21**, 2974 (2001).
26. A. Saras *et al.*, *J. Biol. Chem.* **283**, 10470 (2008).
27. L. H. Tecott, S. L. Smart, in *Comprehensive Textbook of Psychiatry*, B. J. Sadock, V. A. Sadock, Eds. (Lippincott, Williams & Wilkins, New York, ed. 8, 2003), pp. 49–60.
28. Q. Shan, J. L. Haddrill, J. W. Lynch, *J. Biol. Chem.* **276**, 12556 (2001).
29. Single-letter abbreviations for the amino acid residues are as follows: A, Ala; C, Cys; D, Asp; E, Glu; F, Phe; G, Gly; H, His; I, Ile; K, Lys; L, Leu; M, Met; N, Asn; P, Pro; Q, Gln; R, Arg; S, Ser; T, Thr; V, Val; W, Trp; and Y, Tyr.
30. We thank Y. Kohara for *lgc-40*, *lgc-53*, and *lgc-55* cDNA clones, A. Fire for expression vectors, R. O'Hagan for help with electrophysiology, A. Hellman for deletion screening, M. Alkema for discussions, J. Kehoe for bringing to our attention reports of dopamine-activated chloride conductances in mollusks, and D. Denning and B. Galvin for suggestions concerning the manuscript. This work was supported by NIH grant GM24663. N.R. received support from the Howard Hughes Medical Institute, the Life Sciences Research Foundation and The Medical Foundation. H.R.H. is an Investigator of the Howard Hughes Medical Institute.

LXR Regulates Cholesterol Uptake Through Idol-Dependent Ubiquitination of the LDL Receptor

Noam Zelcer,* Cynthia Hong, Rima Boyadjian, Peter Tontonoz†

Cellular cholesterol levels reflect a balance between uptake, efflux, and endogenous synthesis. Here we show that the sterol-responsive nuclear liver X receptor (LXR) helps maintain cholesterol homeostasis, not only through promotion of cholesterol efflux but also through suppression of low-density lipoprotein (LDL) uptake. LXR inhibits the LDL receptor (LDLR) pathway through transcriptional induction of Idol (inducible degrader of the LDLR), an E3 ubiquitin ligase that triggers ubiquitination of the LDLR on its cytoplasmic domain, thereby targeting it for degradation. LXR ligand reduces, whereas LXR knockout increases, LDLR protein levels in vivo in a tissue-selective manner. Idol knockdown in hepatocytes increases LDLR protein levels and promotes LDL uptake. Conversely, adenovirus-mediated expression of Idol in mouse liver promotes LDLR degradation and elevates plasma LDL levels. The LXR-Idol-LDLR axis defines a complementary pathway to sterol response element–binding proteins for sterol regulation of cholesterol uptake.

T he low-density lipoprotein (LDL) receptor (LDLR) is central to the maintenance of plasma cholesterol levels (*1*). Mutations in this receptor are the leading cause of autosomal dominant hypercholesterolemia, characterized by elevated plasma cholesterol levels, and increased risk of cardiovascular disease (*2*, *3*). In line with its pivotal role in cholesterol homeostasis, expression of the LDLR is tightly regulated. Transcription of the *LDLR* gene is coupled to cellular cholesterol levels through the action of the sterol response element–binding protein (SREBP) transcription factors (*4*, *5*). Enhanced processing of SREBPs to their mature forms when cellular sterol levels decline leads to increased *LDLR* transcription (*6*). Posttranscriptional regulation of LDLR expression is also a major determinant of lipoprotein metabolism. Genetic studies have identified mutations in the genes encoding the LDLR adaptor protein 1 (*LDLRAP1/ARH*) (*7*, *8*) and the SREBP target gene proprotein convertase subtilisin/kexin 9 (*PCSK9*) that result in altered stability, endocytosis, or trafficking of the LDLR (*9–13*).

The liver X receptors (LXRs) are also important transcriptional regulators of cholesterol metabolism. LXRα (NR1H3) and LXRβ (NR1H2) are sterol-dependent nuclear receptors activated in response to cellular cholesterol excess (*14*). LXR target genes such as *ABCA1* and *ABCG1* promote the efflux of cellular cholesterol and help to maintain whole-body sterol homeostasis (*15*, *16*). Mice lacking LXRs accumulate sterols in their tissues and manifest accelerated atherosclerosis, whereas synthetic LXR agonists promote reverse cholesterol transport and protect mice against atherosclerosis (*17–19*). The coordinated regulation of intracellular sterol levels by the LXR and SREBP signaling pathways led us to investigate whether LXRs control the uptake as well as efflux of cholesterol.

We initially tested the ability of LXRs to modulate LDL uptake in HepG2 human liver cells and primary mouse macrophages (*20*). Treatment with synthetic LXR ligand (GW3965 or T1317) decreased binding and uptake of boron-dipyrromethene (BODIPY)-labeled LDL (Fig. 1A). The LXR ligands modestly induced changes in LDLR mRNA expression (fig. S1A); however, they decreased LDLR protein levels rapidly and in a dose-dependent manner, and this effect was independent of cellular sterol levels (Fig. 1, B to D). Levels of ABCA1 protein, an established target of LXR, were reciprocally increased by LXR ligands (Fig. 1, B to D). LXR ligands had no effect on LDLR levels in macrophages or mouse embryonic fibroblasts (MEFs) lacking LXRα and LXRβ (Fig. 1E and fig. S1B). LXR activation also decreased LDLR protein but not mRNA levels in human SV589 fibroblasts (fig. S1, C and D) (*21*).

To investigate the link between endogenous LXR ligands and LDLR expression, we used an adenovirus vector encoding oxysterol sulfotransferase (Sult2b1) (*22*, *23*). Depletion of oxysterol agonists by Sult2b1 in SV589 cells led to increased LDLR protein, and this effect was reversed by synthetic ligand (fig. S1E). We further tested the effect of LXR agonists on LDLR produced from a transfected vector (i.e., not subject to endogenous SREBP regulation). In HepG2 cells stably expressing an LDLR–green fluorescent protein (GFP) fusion protein, LDLR-GFP expression was localized primarily on the plasma membrane (Fig. 1F). Ligand activation of LXR decreased LDLR-GFP

Howard Hughes Medical Institute and Department of Pathology and Laboratory Medicine, University of California, Los Angeles (UCLA), Los Angeles, CA 90095, USA.

*Present address: Division of Biopharmaceutics, Leiden/Amsterdam Center for Drug Research, Gorlaeus Laboratories, Leiden University, P.O. Box 9502, 2300RA Leiden, Netherlands.
†To whom correspondence should be addressed. E-mail: ptontonoz@mednet.ucla.edu

levels and redistributed the protein from the plasma membrane to intracellular compartments.

To investigate the mechanism by which LXR affects the LDLR, we examined LXR target genes by transcriptional profiling. We identified a potential mediator, denoted on our array as 9430057C20Rik (table S1), that corresponds to a protein originally identified on the basis of its interaction with myosin regulatory light chain (24). We propose that this protein, which has been variably referred to as Mir and Mylip, be renamed Idol (for inducible degrader of the LDLR) to reflect its biologic function. Idol contains a band 4.1 and Ezrin/Radixin/Moesin homology (FERM) domain that mediates interactions with cytoplasmic domains of transmembrane proteins (25, 26). Unique among FERM domain-containing proteins, Idol also contains a C-terminal RING domain and has been proposed to act as an E3 ubiquitin ligase, although its biological substrate(s) have not been identified (24, 27). Idol mRNA is widely expressed in mice in vivo (fig. S2A). Exposure of cells to increasing concentrations of LDL induced the expression of both Idol and Abca1 mRNA, indicating that their expression is responsive to extracellular cholesterol levels (fig. S2B). Furthermore, LXR agonists induced Idol expression in multiple cells in an LXR-dependent manner, including primary hepatocytes, primary macrophages, MEFs, and HepG2 cells (Fig. 2A and fig. S2, C to E). Treatment of mice with GW3965 induced expression of Idol in multiple tissues, including the spleen, intestine, and adrenals (Fig. 2B). Only modest regulation of Idol by LXR agonist was observed in liver, consistent with the degree of Abca1 regulation (fig. S2F). Idol mRNA levels were also substantially decreased in the spleen and liver of $Lxr\alpha\beta^{-/-}$ mice compared with those of wild-type (WT) controls (fig. S2G).

LXR regulation of Idol was not sensitive to cycloheximide, suggesting that it was a direct transcriptional effect (fig. S3A). It was not secondary to induction of SREBP-1c, because oxysterols that block SREBP processing still induced Idol expression (fig. S3B). LXRs activate target genes by binding to consensus elements (LXREs) in their promoters. We identified an LXRE ~2.5 kilobases upstream of the mouse Idol translation start site (fig. S3C) and generated a reporter construct encompassing this region. Activation by LXRα and GW3965 resulted in a roughly four-fold increase in reporter activity that was largely abolished in the absence of a functional LXRE (fig. S3D). Electromobility shift analysis showed that LXR/RXR bound to WT but not mutant versions of the Idol LXRE (fig. S3E).

Given that Idol is a putative E3 ubiquitin ligase, we hypothesized that Idol induction might underlie the ability of LXRs to regulate LDLR abundance. Using a cotransfection system in human embryonic kidney (HEK) 293T cells, we found that Idol expression redistributed LDLR-GFP from the plasma membrane to an intracellular compartment (Fig. 2C) and reduced the level of LDLR-GFP protein in a dose-dependent

manner (Fig. 2D). Even levels of Idol protein too low to be detected by our antibody were effective. In contrast, Idol carrying a point mutation [Cys^{387} → Ala^{387} (C387A)] in the catalytic RING domain (27) had no effect on the LDLR (Fig. 2C and fig. S4A). Idol levels are very low, even when driven from an exogenous vector, suggesting that Idol is an unstable protein. In support of this idea, Idol levels were greatly enhanced when the RING domain was mutated, raising the possibility that Idol might catalyze its own degradation (fig. S4A).

The effect of Idol on membrane proteins appears to be selective for the LDLR. Levels of transfected LRP1-GFP or β-amyloid precursor protein–GFP proteins, both of which undergo regulated endocytosis similar to the LDLR, were unaffected by Idol expression (fig. S4A). Similarly, Idol did not influence protein levels of

ABCA1-GFP, endogenous transferrin receptor, endogenous myosin regulatory light chain, or the LDLR family members Lrp4 and SorLA (fig. S4, A and B). The very closely related family member ApoER2 was marginally affected by Idol. Adenovirus-mediated expression of Idol reduced LDLR protein levels in primary hepatocytes, HepG2 cells, and McR-H7777 rat hepatocytes (Fig. 2E) and also reduced LDL uptake in MEFs and McR-H7777 cells (Fig. 2F).

To explore the role of endogenous Idol in LDLR regulation, we developed short hairpin RNAs (shRNAs) targeting Idol (fig. S5). Idol-specific shRNAs increased LDLR protein levels in MEFs (Fig. 3A) and McR-H7777 cells (Fig. 3B) without affecting LDLR or LXR or SREBP2 target mRNAs (Fig. 3C and fig. S5), suggesting that Idol activity is a physiological mechanism for reg-
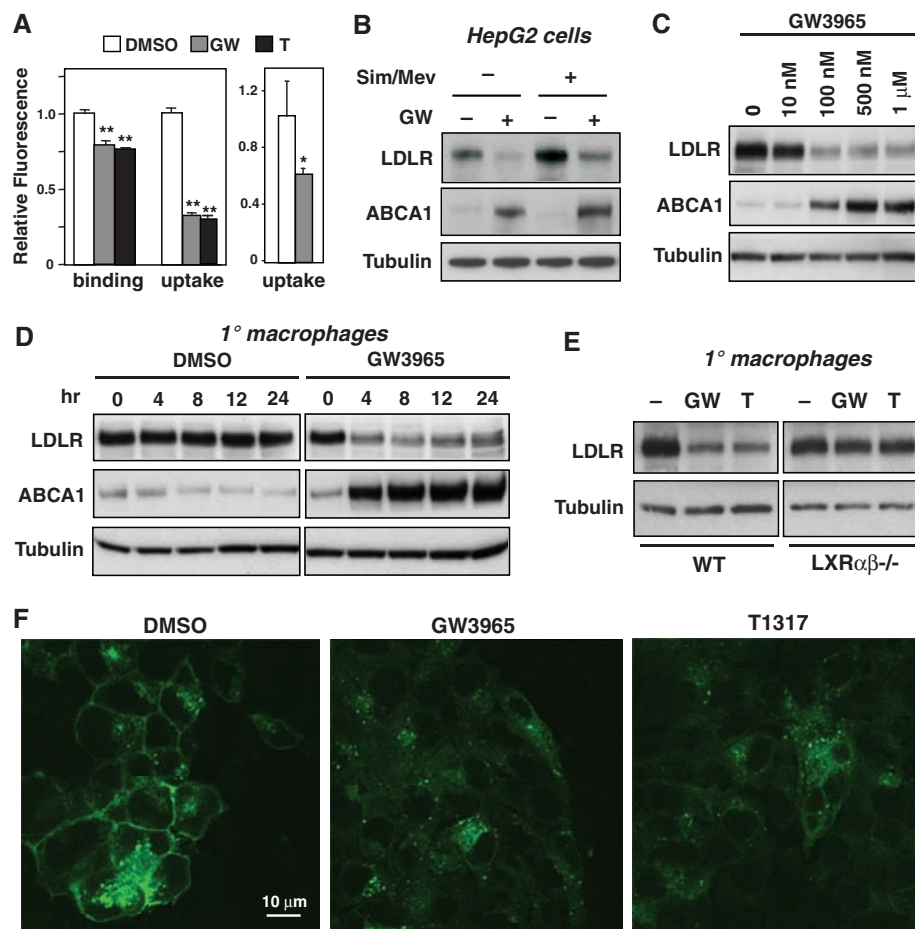

Fig. 1. Activation of LXR inhibits LDL uptake through reduction in LDLR protein expression. (**A**) BODIPY-LDL binding and uptake in HepG2 cells (left) and mouse peritoneal macrophages (right) treated with dimethyl sulfoxide (DMSO) or the synthetic LXR ligands GW3965 (GW) and T0901317 (T) (n = 6 animals per group). *P < 0.05; **P < 0.01. Error bars in this and all subsequent figures represent the mean ± SD. (**B**) HepG2 cells were pretreated with DMSO or GW (1 μM) for 8 hours and subsequently grown in lipoprotein-deficient serum (LPDS) or in sterol-depletion medium (LPDS supplemented with 5 μM simvastatin and 100 μM mevalonic acid) containing either DMSO or GW for an additional 18 hours. (**C**) Primary mouse peritoneal macrophages were cultured in sterol-depletion medium and treated with indicated doses of GW for 8 hours. (**D**) Peritoneal macrophages were cultured in sterol-depletion medium and treated with GW (1 μM) for the indicated time. (**E**) Peritoneal macrophages from WT or $Lxr\alpha\beta^{-/-}$ mice were cultured in sterol-depletion medium and treated with LXR ligands. (**F**) Immunofluorescence images of HepG2 cells stably expressing LDLR-GFP treated with DMSO, GW, or T (1 μM) for 72 hours. All blots are representative of at least three independent experiments.
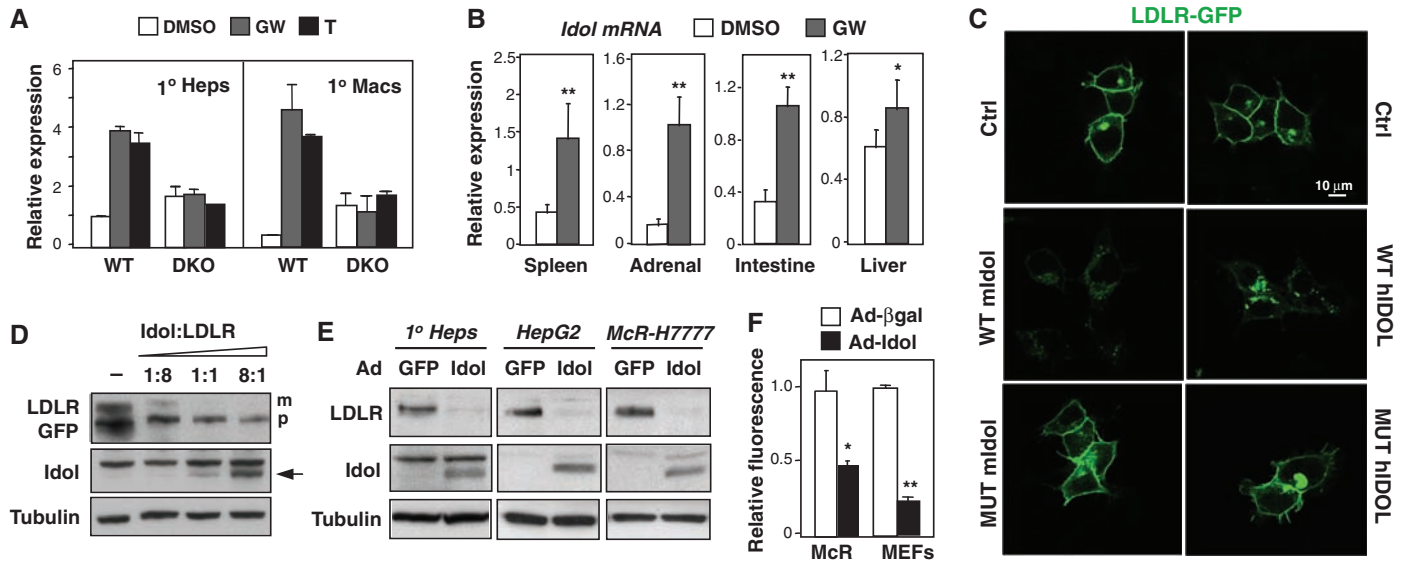
Fig. 2. The LXR target gene Idol is a regulator of LDLR protein levels. (**A**) LXR-dependent regulation of Idol in primary mouse hepatocytes and peritoneal macrophages after treatment with GW or T (1 μM). DKO, LXR double knockout. (**B**) Induction of Idol mRNA expression in tissues of mice treated with 40 mg/kg GW3956 by oral gavage for 3 days (n = 6 per group). Gene expression was measured by real-time PCR. (**C**) Immunofluorescence images of HEK293 cells cotransfected with LDLR-GFP and either WT or RING domain mutant human and mouse Idol. (**D**) Dose-dependent reduction of LDLR-GFP protein in HEK293 cells cotransfected with mIdol and LDLR-GFP expression plasmids. Total cell lysates were analyzed by immunoblotting. Arrow indicates the Idol protein. (**E**) Primary hepatocytes, HepG2 cells, or McR-H7777 cells were cultured in sterol-depletion medium and infected with Ad-GFP or Ad-Idol. Total cell lysates were analyzed by immunoblotting. (**F**) BODIPY-LDL uptake in McR-H777 (McR) cells and LXRα MEFs after infection with Ad-βgal or Ad-Idol (n = 3). All blots are representative of at least three independent experiments. *P < 0.05; **P < 0.01.

ulating LDLR abundance. In support of this idea, Idol-specific shRNAs increased LDL uptake in both fibroblasts (Fig. 3D) and McR-H7777 cells (Fig. 3E). Finally, the ability of an LXR ligand to reduce LDLR protein levels was diminished by Idol shRNA, implicating Idol in LXR-dependent regulation of the LDLR (Fig. 3F).

Pulse-chase labeling studies showed that Idol did not block *LDLR* mRNA translation or appearance of the immature protein, but it completely prevented appearance of the mature glycosylated form (Fig. 4A). Given that mutation of the RING domain inactivates Idol, the most parsimonious explanation for our data is that Idol acts as an E3 ligase to trigger ubiquitination of the LDLR itself, thereby marking it for degradation. We found that ubiquitination of transfected LDLR in 293T cells was dramatically enhanced by expression of active but not mutant Idol (Fig. 4B). Analysis of a series of LDLR receptor mutants that become trapped at various stages of the maturation or recycling pathway revealed that Idol is capable of acting in the endoplasmic reticulum (ER). LDLR [Gly^{546} → Asp^{546} (G546D)], which is unable to exit the ER (28), could still be degraded by Idol (Fig. 4C). Treatment of cells with brefeldin A, which blocks protein trafficking out of the ER, did not inhibit ubiquitination of the WT LDLR (fig. S6A) or the G546D mutant (fig. S6B). Treatment with ammonium chloride, a disruptor of lysosomal pH, inhibited LXR-induced endogenous LDLR degradation (fig. S6C). These data suggest that Idol can ubiquitinate the precursor LDLR in the ER and that subsequent trafficking to the lysosome is required for degradation. We also observed LXR ligand-
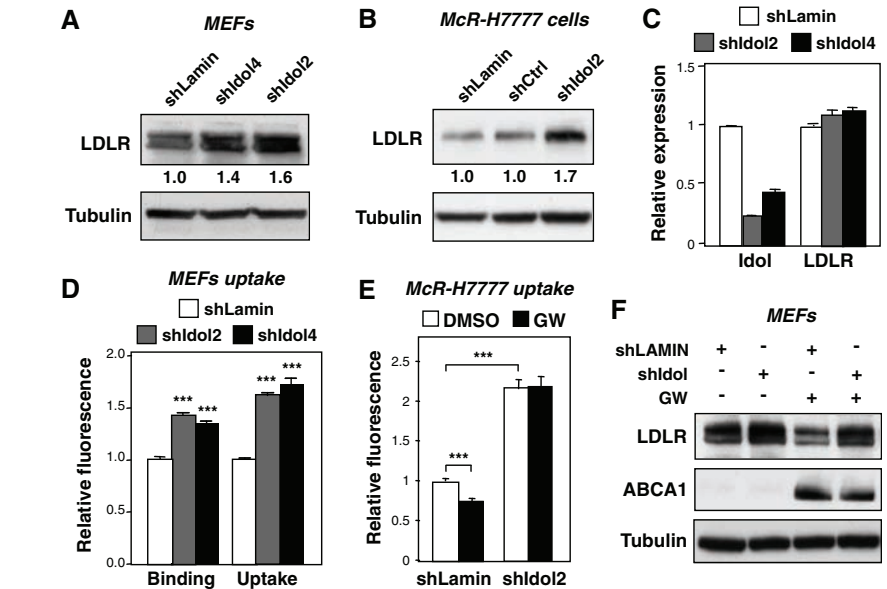

Fig. 3. Idol knockdown induces LDLR protein expression and promotes LDL uptake. (**A**) LXRα MEFs were infected with control (shLamin) or two independent adenoviral Idol shRNA constructs and cultured in sterol-depletion medium. Cell lysates were analyzed by immunoblotting. (**B**) Immunoblot analysis of lysates from McR-H7777 cells treated as in (A). (**C**) Gene expression was analyzed by real-time PCR in LXRα MEFs treated as in (A). (n = 3). (**D**) BODIPY-LDL binding and uptake was determined for LXRα MEFs after infection with Ad-shLAMIN, Ad-shIdol2, or Ad-shIdol4 (n = 3). (**E**) BODIPY-LDL uptake was determined for McR-H7777 cells after infection with Ad-shLAMIN or Ad-shIdol2 followed by treatment with DMSO or GW (1 μM) as indicated (n = 4). (**F**) LXRα MEFs were infected with Ad-shLAMIN or Ad-shIdol2 for 24 hours. Subsequently, cells were treated with DMSO or GW followed by culture in sterol-depletion medium. All blots are representative of at least three independent experiments. ***P < 0.001.

dependent ubiquitination of endogenous LDLR in primary macrophages (Fig. 4D) and Idol-dependent ubiquitination of endogenous LDLR in primary

hepatocytes (Fig. 4E). GW3965 triggered LDLR ubiquitination within 4 hours, consistent with the time course of LDLR degradation (Figs. 1D and 4D).

Fig. 4. Idol reduces LDLR protein expression through ubiquitination of conserved residues in its cytoplasmic domain. (**A**) 24 hours after infection with Ad-LacZ or Ad-Idol HepG2-LDLR-GFP, cells were pulsed with [^{35}S]methionine and [^{35}S]cysteine for 15 min and chased as indicated. Samples were immunoprecipitated at the indicated time points after labeling. (**B**) HEK293 cells were cotransfected with LDLR-GFP, Idol, and HA-ubiquitin expression plasmids. After 36 hours, lysates were subjected to immunoprecipitation (IP) and immunoblotting. HA, hemagglutinin; Ub, ubiquitin; WB, Western blot. (**C**) Total HEK293 cell lysates were analyzed by immunoblotting 48 hours after cotransfection with Idol and WT or mutant LDLR expression plasmids. p, immature protein; m, mature glycosylated form. (**D**) Peritoneal macrophages were cultured in sterol-depletion medium and treated with 1 μM GW3965 for 4 hours. Total lysates were immunoprecipitated with anti-ubiquitin, then immunoblotted (IB) for LDLR. (**E**) Primary mouse hepatocytes were infected with Ad-GFP or Ad-Idol and cultured in sterol-depletion medium. After 24 hours, lysates were immunoprecipitated with anti-ubiquitin antibody and then immunoblotted for LDLR. (**F**) Evolutionary conservation of the LDLR intracellular domain. Potential ubiquitination sites are indicated. (**G**) Immunoblot analysis of HEK293 total cell lysates cotransfected with control or Idol expression plasmids along with the indicated mutated LDLR constructs. Numbering in the LDLR constructs refers to Fig. 1F. (**H**) HEK293 cells were cotransfected with LDLR, mutant LDLR (K6R/K20R/C29A), Idol, and HA-ubiquitin expression plasmids as indicated. Subsequently, cells were treated with vehicle or 25 μM MG132 for 6 hours. Blots are representative of at least two independent experiments. IgG, immunoglobulin G.
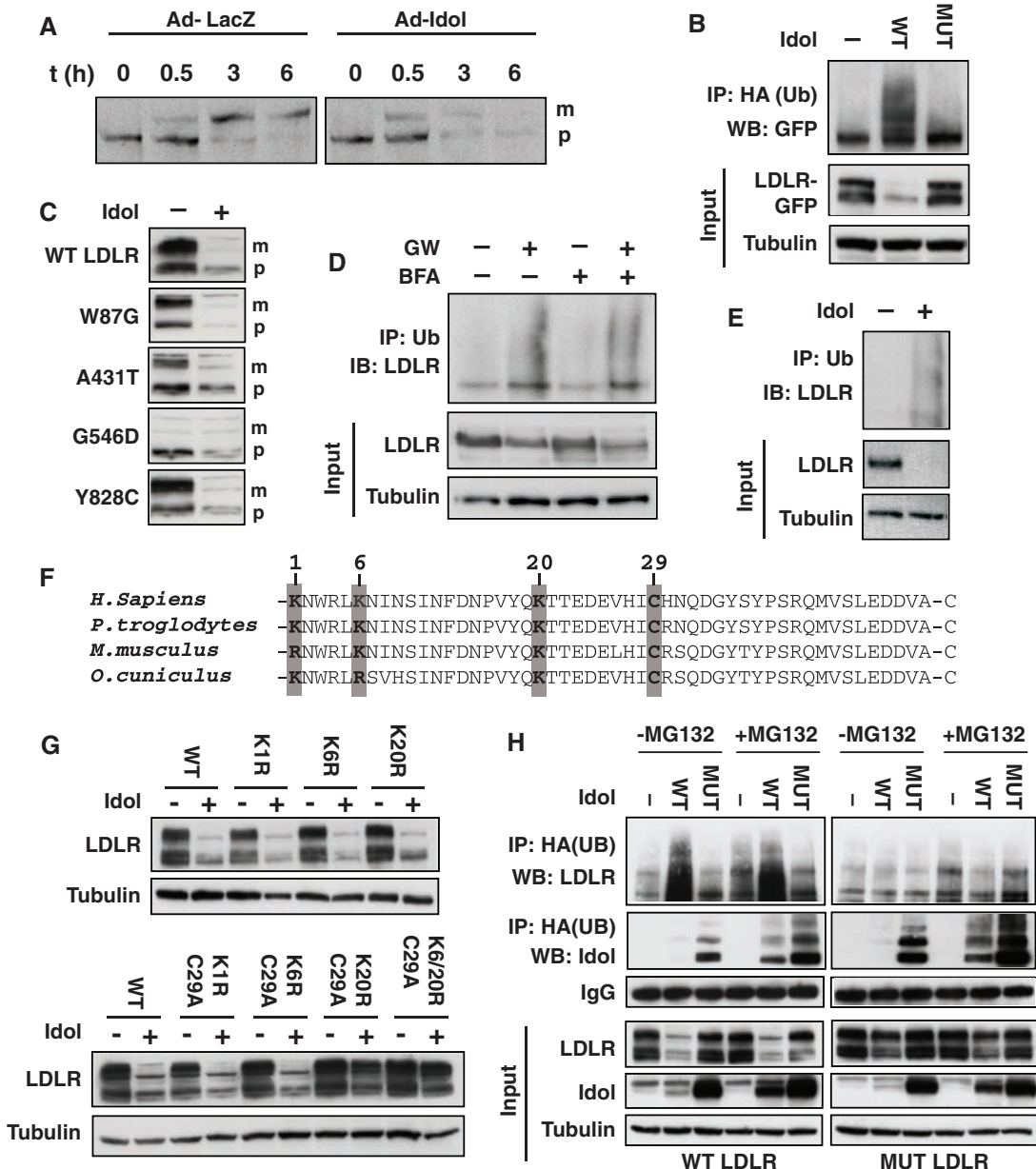
We determined the structural requirements for Idol-dependent LDLR degradation with the use of mutational analysis. Idol had no effect on an LDLR lacking the entire 50–amino acid intracellular domain (fig. S6D). The LDLR intracellular domain contains three highly conserved lysine residues and one cysteine that could be potential sites for ubiquitination (Fig. 4F) (*29*). Single mutations of any of these residues, or combined mutation of all three lysine residues, did not prevent Idol from degrading the LDLR (Fig. 4G and fig. S6E). However, superimposing a cysteine mutation on constructs containing two or three mutated lysines rendered the LDLR insensitive to degradation. Additional mutagenesis revealed that either an intact Lys^{20} (K20) or an intact Cys^{29}

(C29) was required for Idol-mediated degradation (Fig. 4G and fig. S6E). Finally, not only did combined mutation of the K20 and C29 residues block LDLR degradation by Idol, it also blocked ubiquitination (Fig. 4H). The proteasome blocker MG132, despite stabilizing Idol protein, did not stabilize the LDLR, consistent with previous reports that degradation of the LDLR occurs in the lysosome (Fig. 4H) (*30*, *31*).

To investigate whether activation of the LXR-Idol pathway affects LDLR expression in vivo, we treated mice with GW3965. LXR agonist reduced LDLR protein levels in a tissue-selective manner, concordant with the degree of Idol induction (Figs. 2B and 5A). Whereas prominent effects were observed in intestine and peritoneal

macrophages, LXR ligand had minimal effect on Idol mRNA and LDLR protein levels in the liver. Notably, we observed a reciprocal effect on LDLR protein levels in resident macrophages and intestine when we analyzed mice in which the LXR-Idol pathway is inactive (Fig. 5B). LDLR protein levels were substantially higher in macrophages and intestine of LXRαβ$^{-/-}$ mice as compared with WT controls. LDLR levels were also slightly higher in the liver. Thus, gain or loss of LXR-Idol activity affects LDLR expression in vivo.

Because Idol was not subject to strong LXR regulation in the liver, we employed an alternative strategy to test its function in this tissue. We infected mice with adenoviral vectors encoding β-galactosidase or mouse Idol. Idol expression

Fig. 5. Idol expression regulates LDLR expression and affects plasma cholesterol and LDL levels in vivo. (**A**) C57BL/6 mice were treated for 3 days with 40 mg/kg per day GW3965 by oral gavage. Total lysates from resident peritoneal macrophages, small intestine (ileum), and liver were analyzed for protein levels by immunoblotting. Macrophages were isolated from the peritoneal cavity and processed without in vitro culture. (**B**) Total lysates from macrophages, small intestine (ileum), and liver from WT and $Lxr\alpha\beta^{-/-}$ mice were analyzed by immunoblotting. Macrophages were isolated from the peritoneal cavity and processed without in vitro culture. (**C**) Analysis of plasma cholesterol 6 days after transduction of C57BL/6 mice with Ad-β-gal or Ad-Idol. ($n = 8$ mice per group) ***$P < 0.001$. (**D**) Cholesterol content of size-fractionated lipoproteins from mice infected with Ad-β-gal or Ad-Idol. (**E**) Immunoblot analysis of total liver lysates. Data are representative of at least two independent experiments.
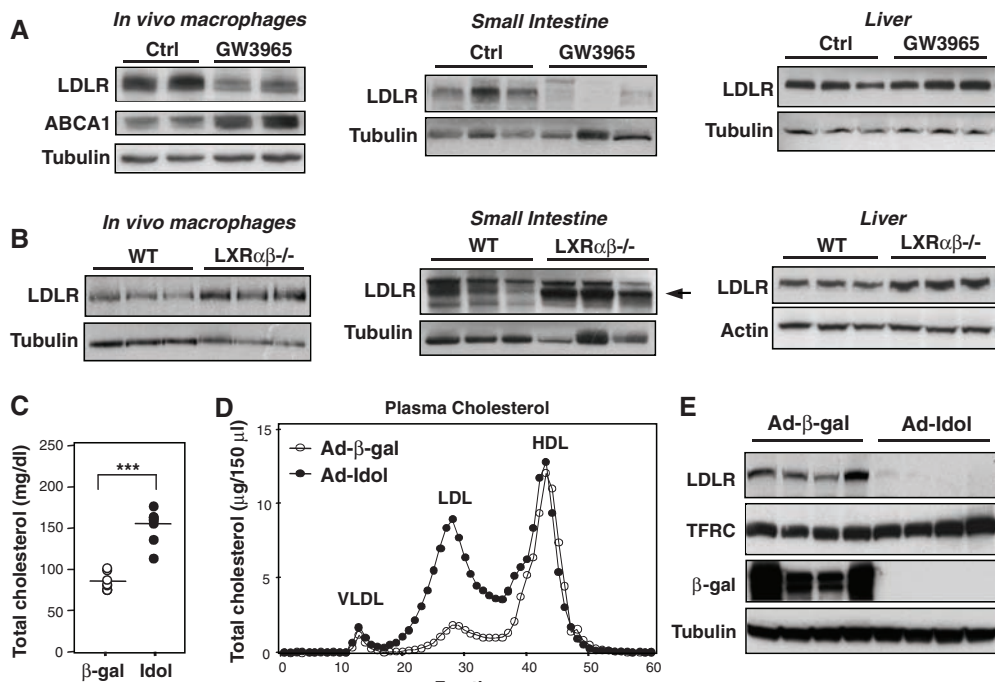
increased plasma levels of total and unesterified cholesterol, whereas levels of triglycerides, free fatty acids, and glucose were not significantly altered (Fig. 5C and fig. S7A). Fractionation of plasma lipoproteins revealed that Idol expression caused a phenotype reminiscent of that exhibited by $Ldlr^{(-/-)}$ mice, with the appearance of a prominent LDL peak not present in the control mice (Fig. 5D and fig. S7B). Plasma apoB protein levels were increased by approximately threefold in Idol-transduced mice, and there was no difference in PCSK9 levels (fig. S7, C and D). Consistent with our in vitro results, hepatic expression of LXR and SREBP-2 target genes was not affected by Idol expression (fig. S7E), but LDLR protein levels were markedly reduced (Fig. 5E). In contrast, transferrin receptor levels were not altered by Idol. Finally, Idol adenovirus had no effect on plasma cholesterol levels (fig. S8A) or lipoprotein profiles (fig. S8B) in $Ldlr^{(-/-)}$ mice, demonstrating that Idol requires LDLR expression for these effects.

In summary, we have shown that the sterol-sensitive nuclear receptor LXR regulates LDLR-dependent cholesterol uptake through a pathway independent of the SREBPs. LXR induces the expression of Idol, which in turn catalyzes the ubiquitination of the LDLR, thereby targeting it for degradation. These results provide a potential explanation for an earlier observation that an ectopically expressed LDLR could still be regulated by sterols (32). Identification of the Idol-LDLR pathway fills a gap in our understanding of how LXRs control cholesterol homeostasis. The ability of LXRs to respond to excess cellular cholesterol by promoting efflux through ABC transporters has been extensively documented (14). The LXR-Idol-LDLR pathway provides a mechanism to simultaneously limit LDL cholesterol uptake. Idol and ABCA1 are coordinately regu-

lated by LXR in a cell-type selective manner, consistent with this functional link.

The LXR-Idol pathway appears to be most active in peripheral cells such as macrophages, adrenals, and intestine. At the same time, however, Idol is constitutively expressed in the liver, and gain or loss of Idol function in cultured hepatocytes regulates LDLR protein levels and affects LDL uptake. Forced expression of Idol in liver in vivo profoundly reduces LDLR levels, further indicating that Idol is capable of degrading LDLR in this tissue.

Whether Idol expression is required for LDLR degradation in vivo is a critical question that remains to be addressed. If it is required, then conceivably the Idol pathway could be targeted pharmacologically so as to increase LDLR levels and enhance LDL clearance.

References and Notes

1. D. W. Russell *et al.*, *Cell* **37**, 577 (1984).
2. H. Tolleshaug, K. K. Hobgood, M. S. Brown, J. L. Goldstein, *Cell* **32**, 941 (1983).
3. M. S. Brown, J. L. Goldstein, *Science* **232**, 34 (1986).
4. C. Yokoyama *et al.*, *Cell* **75**, 187 (1993).
5. X. Hua *et al.*, *Proc. Natl. Acad. Sci. U.S.A.* **90**, 11603 (1993).
6. J. L. Goldstein, R. A. DeBose-Boyd, M. S. Brown, *Cell* **124**, 35 (2006).
7. C. K. Garcia *et al.*, *Science* **292**, 1394 (2001); published online 26 April 2001 (10.1126/science.1060458).
8. J. C. Cohen, M. Kimmel, A. Polanski, H. H. Hobbs, *Curr. Opin. Lipidol.* **14**, 121 (2003).
9. M. Abifadel *et al.*, *Nat. Genet.* **34**, 154 (2003).
10. J. Cohen *et al.*, *Nat. Genet.* **37**, 161 (2005).
11. N. G. Seidah *et al.*, *Proc. Natl. Acad. Sci. U.S.A.* **100**, 928 (2003).
12. K. N. Maxwell, J. L. Breslow, *Proc. Natl. Acad. Sci. U.S.A.* **101**, 7100 (2004).
13. S. W. Park, Y. A. Moon, J. D. Horton, *J. Biol. Chem.* **279**, 50630 (2004).
14. N. Zelcer, P. Tontonoz, *J. Clin. Invest.* **116**, 607 (2006).
15. J. J. Repa *et al.*, *Science* **289**, 1524 (2000).
16. M. A. Kennedy *et al.*, *Cell Metab.* **1**, 121 (2005).
17. D. J. Peet *et al.*, *Cell* **93**, 693 (1998).
18. R. K. Tangirala *et al.*, *Proc. Natl. Acad. Sci. U.S.A.* **99**, 11896 (2002).
19. S. B. Joseph *et al.*, *Proc. Natl. Acad. Sci. U.S.A.* **99**, 7604 (2002).
20. Materials and methods are available as supporting material on *Science* Online.
21. C. M. Adams *et al.*, *J. Biol. Chem.* **279**, 52772 (2004).
22. W. Chen, G. Chen, D. L. Head, D. J. Mangelsdorf, D. W. Russell, *Cell Metab.* **5**, 73 (2007).
23. S. J. Bensinger *et al.*, *Cell* **134**, 97 (2008).
24. P. A. Olsson, L. Korhonen, E. A. Mercer, D. Lindholm, *J. Biol. Chem.* **274**, 36288 (1999).
25. R. A. Anderson, R. E. Lovrien, *Nature* **307**, 655 (1984).
26. A. Bretscher, K. Edwards, R. G. Fehon, *Nat. Rev. Mol. Cell Biol.* **3**, 586 (2002).
27. B. C. Bornhauser, C. Johansson, D. Lindholm, *FEBS Lett.* **553**, 195 (2003).
28. H. H. Hobbs, D. W. Russell, M. S. Brown, J. L. Goldstein, *Annu. Rev. Genet.* **24**, 133 (1990).
29. K. Cadwell, L. Coscoy, *Science* **309**, 127 (2005).
30. K. N. Maxwell, E. A. Fisher, J. L. Breslow, *Proc. Natl. Acad. Sci. U.S.A.* **102**, 2069 (2005).
31. D. W. Zhang *et al.*, *J. Biol. Chem.* **282**, 18602 (2007).
32. M. F. Sharkey, A. Miyanahara, R. L. Elam, T. Friedmann, J. L. Witztum, *J. Lipid Res.* **31**, 2167 (1990).
33. We thank members of the Tontonoz and Edwards laboratories and J. Wohlschlegel, P. Edwards, and S. G. Young for fruitful discussions. We thank P. Tarr for assistance with confocal microscopy, K. Matter and A. Gonzalez for LDLR plasmids, and I. Koster for critically reading the manuscript. N.Z. was supported by a long-term postdoctoral fellowship from the Human Frontier Science Program Organization. P.T. is an investigator of the Howard Hughes Medical Institute. This work was also supported by NIH grants HL066088, HL090553, and HL030568. UCLA and two of the authors (N.Z. and P.T.) have filed a patent related to this work.